Bombesin-Targeted PET of Prostate Cancer

Rosalba Mansi*[1], Ryogo Minamimoto*[2], Helmut Mäcke[1], and Andrei H. Iagaru[3]

[1]Department of Nuclear Medicine, University Hospital of Freiburg, Freiburg, Germany; [2]Division of Nuclear Medicine, Department of Radiology, National Center for Global Health and Medicine, Tokyo, Japan; and [3]Division of Nuclear Medicine and Molecular Imaging, Department of Radiology, Stanford University, Stanford, California

Imaging plays an important role in prostate cancer (PC), including accurate evaluation of the extent of disease, assessment of sites of recurrent disease, and monitoring of response to treatment. Molecular imaging techniques are among the novel developments related to the imaging of PC, and various SPECT and PET radiopharmaceuticals are now available in clinical trials or commercially. Here we describe the preclinical and clinical use of gastrin-releasing peptide receptors as targets for the imaging of PC, with a focus on the development of PET tracers for the imaging of gastrin-releasing peptide receptor–positive tumors.

Key Words: bombesin; prostate; cancer; PET

Prostate cancer (PC) is the most common malignancy in men, accounting for 29% of all tumors, and is the second most common cause of cancer-related deaths in the same population. The American Cancer Society estimates that there will be 180,890 new cases of PC and 28,170 deaths because of it in 2016 (1). In this review, we discuss the preclinical and clinical work already done or under evaluation for the use of gastrin-releasing peptide receptors (GRPRs) as targets for the imaging of PC, with a focus on the development of PET tracers for the imaging of GRPR-positive tumors. Comprehensive recent reviews have discussed tracers for use in SPECT and therapy (2,3).

PRECLINICAL AND TRANSLATIONAL DEVELOPMENTS

GRPRs are G protein–coupled receptors overexpressed in a variety of major human cancers, such as PC and breast and small cell lung cancers, as well as in the tumoral vessels of urinary tract cancers (4). They belong to the bombesin receptor family, which has various physiologic functions in the gastrointestinal tract and nervous system (5). Bombesin is a 14-mer peptide (Pyr-Gln-Arg-Leu-Gly-Asn-Gln-Trp-Ala-Val-Gly-His-Leu-Met-NH$_2$) that binds with a high affinity to GRPR (5).

GRPR AGONISTS

Because of the overexpression of GRPR in human cancers, efforts have been focused on the development of radiolabeled bombesin-based peptides for imaging and therapy. The main focus of such translational developments was on PC. GRPR expression was identified on the messenger RNA level as well as on the protein level of primary PC and metastases. Markwalder and Reubi (6) showed that GRPR expression depended on the Gleason score, with higher receptor levels at low Gleason scores (3–6) and lower receptor levels at high Gleason scores (7–9). Early GRPR ligand developments and studies in preclinical models focused on agonists because of their known property of internalization when bound to the receptors. A minimal amino acid sequence, bombesin residues 7–14, was shown to have high binding affinity and agonist potency. A summary of positron emitters used to label PET radiopharmaceuticals targeting GRPR is shown in Table 1.

^{68}Ga was first used to label GRPR agonists for clinical translation. Modifications of the pharmacokinetic profile to enhance metabolic stability, tumor uptake, and image contrast are still ongoing and successful (7,8). Despite extensive studies, only 2 peptides have been translated clinically: ^{68}Ga-BZH3 (in patients with gliomas and gastrointestinal stromal tumors) (9,10) and ^{68}Ga-AMBA (in patients with various cancers) (11). Carlucci et al. described the development of ^{18}F-labeled bombesin analogs (12).

GRPR ANTAGONISTS

The important finding that somatostatin receptor antagonists are superior to agonists as imaging and targeted radionuclide agents and the short-term adverse effects of GRPR agonists have resulted in interest in antagonists of the bombesin receptor family.

Typical modifications of the agonistic truncated octapeptide are shown in Figure 1. The statine-based JMV594 (DPhe-Gln-Trp-Ala-Val-Gly-His-Sta-Leu-NH$_2$) is, by far, the most studied GRPR antagonist for the imaging and therapy of PC to date. Originally developed by Llinares et al. (13), JMV594 was first modified by adding different spacers and chelators to make it suitable for labeling with several radiometals for PET, SPECT, and therapy. Mansi et al. (14) reported the first PET statine-based bombesin receptor antagonist, RM1 (DOTA-Gly-aminobenzoic acid-DPhe-Gln-Trp-Ala-Val-Gly-His-Sta-Leu-NH$_2$), in which JMV594 was modified by the addition of glycine-4-aminobenzoyl and the chelator DOTA to allow complexation with 3+ radiometals. PET imaging of ^{68}Ga-DOTA-RM1 in PC-3 xenografts confirmed the high-level and specific accumulation of the radiotracer in the tumors and GRPR-positive organs. The addition of the positively charged spacer 4-amino-1-carboxymethyl-piperidine led to RM2

TABLE 1
Physical Properties of PET Radionuclides Used to Label Bombesin Analogs

Characteristic	[68]Ga	[64]Cu	[18]F
Half-life	67.7 min	12.7 h	109.7 min
Decay	β^+: 89%	β^+: 17.8%	β^+: 97%
	EC: 11%	β^-: 38.4%	EC: 3%
		EC: 43.8%	
$E_{\beta\text{-max}}$ (keV)	1,880	656	635
Production	Generator	Cyclotron	Cyclotron
Oxidation state	3+	2+ (1+)	1−

and therapy (theragnostics) is based mainly on [68]Ga–[177]Lu (^{177}Lu) and [68]Ga–[90]Y (^{90}Y) pairs. Nevertheless, ^{18}F-labeled radiotracers provided good tumor visualization and may be preferred because of the superior imaging characteristics of [18]F. Moreover, the availability of larger tracer activity amounts and the relatively long half-life of ^{18}F enable centralized production and commercial distribution to small or remote imaging centers, as well as imaging at later time points, resulting in a higher level of clearance and a lower level of nonspecific binding.

Gourni et al. (20) studied the peptide–chelator conjugate MJ9 (H-4-amino-1-carboxymethyl-piperidine-DPhe-Gln-Trp-Ala-Val-Gly-His-Sta-Leu-NH₂) coupled to NOTA and radiolabeled with ^{68}Ga, resulting in a final 1+ charge (^{68}Ga-NOTA-MJ9). They reported that ^{68}Ga-NOTA-MJ9 had a higher binding affinity and a longer retention time than neutral complexes ^{68}Ga-NODAGA-MJ9 (NODAGA: 1,4,7-triazacyclononane,1-glutaric acid) and ^{64}Cu-NOTA-MJ9 and negatively charged ^{64}Cu-NODAGA-MJ9 (20). ^{68}Ga-NODAGA-MJ9 is currently in phase 1 clinical studies. Abiraj et al. (21) compared the same antagonists conjugated to 4 different chelate systems through PEG4 and reported the clear superiority of the positively charged conjugates—namely, ^{64}Cu-CB-TE2A-AR and ^{99m}Tc-N4-AR—over the neutral ones in terms of lower 50% inhibitory concentrations, higher levels of accumulation in the tumors, and longer tumor retention times (Fig. 2). The excellent properties of ^{64}Cu-CB-TE2A-AR resulted in the first clinical studies that successfully demonstrated the feasibility of using statine-based bombesin antagonists for PC detection in humans.

The stability of Cu(II) complexes is an important parameter because Cu²⁺ released in vivo can bind to albumin and accumulate in nontargeted organs, such as the liver. Recently, Gourni et al. (22) chose to couple the Sar chelator—MeCoSar, already used along with somatostatin analogs—to PEG4-JMV594 for Cu(II) complex formation. The chelate had a 2+ charge and was highly stable. The pharmacokinetic properties of this new radiopharmaceutical were excellent and included improved tumor-to-kidney and tumor-to-liver ratios relative to those obtained with ^{64}Cu-labeled bombesin analogs.

(DOTA-4-amino-1-carboxymethyl-piperidine-DPhe-Gln-Trp-Ala-Val-Gly-His-Sta-Leu-NH₂) (15). ^{68}Ga-labeled RM2 was widely studied in different PC cell lines and tumor models and is currently in clinical studies (16,17).

Recently, many research groups worked on the optimization of this class of compounds, investigating the influence of spacers and chelates on binding affinities and pharmacokinetics properties. [18]F, ^{68}Ga, and ^{64}Cu were used to label the statine-based bombesin antagonist through several chelators. Among the different chelators, NOTA (1,4,7-triaza-cyclo-nonane-1,4,7-triacetic acid) and its derivatives were chosen because of the high degree of stability of the complexes they form with various radioisotopes, such as ^{68}Ga, ^{64}Cu, and [18]F. This approach allowed the possibility of side-by-side comparisons with radioconjugates having the same chelator–peptide conjugation and different radiometals. ^{68}Ga-labeled compounds showed better pharmacokinetics overall despite similar uptake in the tumors (18,19). ^{68}Ga-based radiotracers provide sufficient levels of radioactivity for high-quality images in a short scanning time, allowing repeat examinations on the same day. Additionally, the development of radiopharmaceuticals for diagnosis

Another class of bombesin-based receptor antagonists is the C-terminal amide derivative (e.g., [DPhe⁶,Leu-NHEt¹³,des-Met¹⁴]BN(6–14)). This peptide, coupled to DOTA and labeled with ^{68}Ga, was developed by Maina et al. (23) and led to the new radiopharmaceutical ^{68}Ga-DOTA-Sarabesin3. After successful preclinical studies revealing a high binding affinity, good in vivo stability, and excellent targeting efficacy in PC-3 xenografts, this radiotracer exhibited encouraging results in the first clinical study. The same peptide was modified by adding hydrophobic spacers of different lengths (aminohexanoic acid [Ahx₆₋₉]) and functionalized with NOTA for ^{64}Cu complexation (24).

Two additional bombesin receptor antagonist classes, the methyl ester (ARBA05: DOTA-4-amino-1-carboxymethyl-piperidine-DPhe-Gln-Trp-Ala-Val-Gly-His-Leu-OCH₃) and the pseudopeptide (RM7: DOTA-4-amino-1-carboxymethyl-piperidine-DPhe-Gln-Trp-Ala-Val-Gly-His-Leuψ(CHOH-CH₂)-(CH₂)₂-CH₃), were evaluated in a
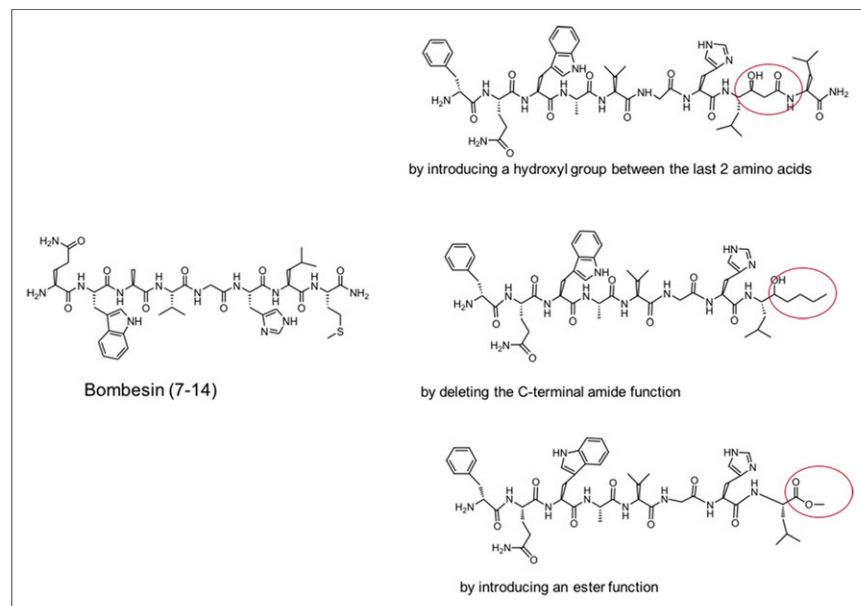

FIGURE 1. Modifications of C-terminal amino acid of bombesin agonist BN(7–14) for design of bombesin receptor antagonists.
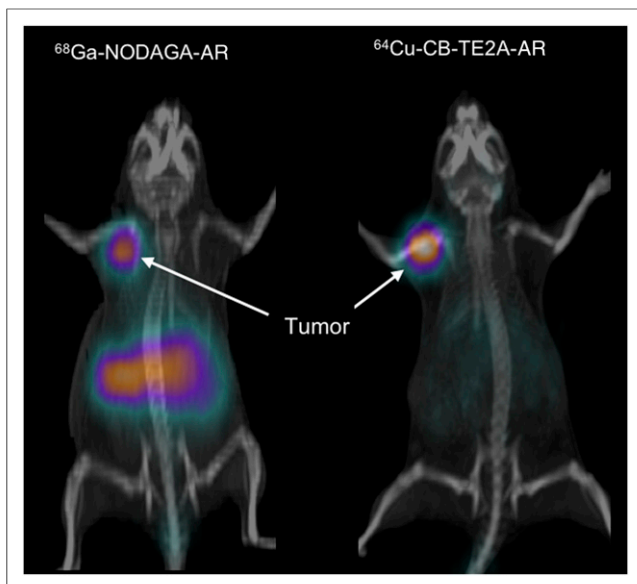
FIGURE 2. PET/CT images obtained for PC-3 tumor–bearing nude mice with ^{68}Ga-NODAGA-AR at 1 h after injection (left) and ^{64}Cu-CB-TE2A-AR at 12 h after injection (right).

direct comparison with ^{68}Ga-RM2 by Mansi et al. (*25*). ^{68}Ga-RM7 had a high binding affinity and excellent pharmacokinetics that rendered it a good candidate for clinical translation.

AGONISTS VERSUS ANTAGONISTS

There is no consensus as to whether agonists or antagonists are preferable for clinical translation. Several studies clearly indicated the superiority of antagonists over agonists. Mansi et al. (*14*) compared the most potent radiolabeled GRPR agonist—AMBA (DO3A-CH$_2$-CO-G-4-aminobenzoyl-Gln-Trp-Ala-Val-Gly-His-Leu-Met-NH$_2$), developed by Lantry et al. (*26*)—with the antagonist RM1. Despite the approximately 10-fold-lower affinity of the antagonist, it had superior pharmacokinetics, showing 3.5-fold-higher tumor uptake as well as distinctly superior tumor-to-background ratios. In addition—and as an explanation for the higher tumor uptake—the authors found a 3-fold-higher number of available binding sites for the antagonist.

Liu et al. (*27*) studied the same 2 peptides (RM1 and AMBA). Instead of DOTA, they used NODAGA for labeling with ^{64}Cu and ^{18}F. They concluded that the antagonist exhibited higher tumor uptake and more favorable pharmacokinetics (*27*), consistent with the results of Mansi et al. (*14*). Another group compared agonistic and antagonistic demobesin and found a distinct advantage for the antagonist (*28*). Conversely, Nanda et al. (*29*) studied ^{64}Cu-NODAGA–conjugated agonists versus antagonists and concluded that the agonist was a superior molecular imaging agent for GRPR targeting. Yang et al. (*30*) studied ^{18}F-labeled GRPR agonists and antagonists and concluded that the agonists performed better than the antagonists. They hypothesized that the superiority found for the radiometal-labeled chelator–conjugated antagonists did not apply to ^{18}F-labeled peptides. There is clearly a need to continue studies to select the ideal targeting agents.

HYBRID PEPTIDES

Promising approaches with hybrid peptides were considered for additional molecular targets besides GRPR. Li et al. (*31*) and Liu et al. (*32*) targeted 2 different receptors, GRPR and integrin $\alpha_v\beta_3$ receptor, and reported favorable pharmacokinetics and enhanced tumor uptake of their ^{18}F- and ^{64}Cu-labeled hybrids, respectively.

Zhou et al. (*33*) developed GRPR-targeted agents conjugated to 2-nitroimidazole moieties as hypoxia-trapping moieties and found increased uptake and retention of the radiotracer in hypoxic cells.

Bandari et al. (*34*) developed the first example of a GRPR–prostate-specific membrane antigen (PSMA) dual targeting ligand for ^{64}Cu labeling and PET imaging. The hybrid bound to both receptors with a high affinity, and PET imaging of 2 tumors expressing the target molecules was able to delineate the tumors.

Kroll et al. (*35*) coupled a GRPR agonist and a GRPR antagonist to a proline scaffold at defined distances along with the chelator DOTA for ^{68}Ga labeling. They aimed at benefiting from the best of the 2 worlds—the agonist world (internalization) and the antagonist world (recognition of a larger number of binding sites). The hybrid peptide was superior to the bivalent agonist and antagonist and had excellent targeting properties.

CLINICAL USE

Up to 40% of PC patients develop biochemical recurrence (BCR) within 10 y after initial treatment (*36*). A detectable or rising prostate-specific antigen (PSA) level after initial therapy is considered BCR or "PSA failure," even when there are no symptoms or signs of locally recurrent or metastatic disease. Usually an increase in the PSA level precedes a clinically detectable recurrence by months to years (*37*). However, it cannot differentiate among local, regional, or systemic disease with the precision essential for further disease management.

Conventional imaging has limited sensitivity and specificity for detecting PC. The sensitivity for the detection of local recurrence ranges from 25% to 54% with transrectal ultrasound or contrast-enhanced CT and is moderately improved with functional MRI techniques (*38*). The sensitivity for the detection of lymph node metastases with CT or MRI has been reported to be 30%–80% (*39*).

Although functional imaging with ^{18}F-FDG PET/CT has limited use in PC (*40,41*), other PET radiopharmaceuticals—such as ^{11}C-choline, ^{11}C-acetate, and ^{18}F-choline—have been evaluated, with good results for detecting PC (*42–46*). Anti-1-amino-3-^{18}F-fluorocyclobutane-1-carboxylic acid, a new synthetic amino acid, may be superior to ^{11}C-choline (*47*). However, a limitation of these PET tracers is the lack of specificity for distinguishing PC from benign prostate hypertrophy, which frequently coexists with PC (*48*). Therefore, different classes of PET radiopharmaceuticals, such as GRPR-targeted agents, may provide information useful in the management of PC. Tables 2 and 3 summarize the clinically translated PET radiopharmaceuticals targeting GRPR.

Dynamic ^{68}Ga-RM2 PET/CT scans obtained for a cohort of 5 healthy men in a pilot study (*17*) indicated that the tracer was rapidly excreted through the kidneys into the urinary bladder, with pancreatic uptake increasing immediately after injection and reaching a plateau 50 min after injection. Maximum peak uptake of the total injected radioactivity was seen in the urinary bladder contents and the liver—approximately 36% and 14%, respectively.

Roivainen et al. (*17*) reported that estimates of the absorbed doses were highest in the urinary bladder wall (0.61 mSv/MBq) and in the pancreas (0.51 mSv/MBq), and the mean effective dose was estimated to be 0.051 mSv/MBq. Regarding the biodistribution of ^{68}Ga-RM2 in normal tissues, the highest uptake was seen in

TABLE 2
Structures of Bombesin Analogs Used in Clinical Trials

Structure	Class	Properties
DPhe-Gln-Trp-Ala-Val-Gly-His-Sta-Leu-NH$_2$	Statine	Antagonist
DPhe-Gln-Trp-Ala-Val-Gly-His-Leu-NHEt	Ethyl amide	Antagonist
DPhe-Gln-Trp-Ala-Val-Gly-His-Leuψ(CHOH-CH$_2$)-(CH$_2$)$_2$-CH$_3$	Pseudopeptide	Antagonist
DPhe-Gln-Trp-Ala-Val-Gly-His-Leu-OCH$_3$	Methyl ester	Antagonist

TABLE 3
Bombesin Compounds Used in Clinical Trials

Compound	Structure
^{68}Ga-RM2	^{68}Ga-DOTA-4-amino-1-carboxymethyl-piperidine-DPhe-Gln-Trp-Ala-Val-Gly-His-Sta-Leu-NH$_2$
^{68}Ga-SB3	^{68}Ga-DOTA-*p*-aminomethylaniline-diglycolic acid-DPhe-Gln-Trp-Ala-Val-Gly-His-Leu-NHEt
^{18}F-BAY-864367	3-cyano-4-^{18}F-fluorobenzoyl-Ala(SO$_3$H)-Ala(SO$_3$H)-Ava-Gln-Trp-Ala-Val-NMeGly-His-Sta-Leu-NH$_2$
[64]Cu-CB-TE2A-AR06	^{64}Cu-CB-TE2A-PEG4-DPhe-Gln-Trp-Ala-Val-Gly-His-Sta-Leu-NH$_2$

the pancreas, kidneys, and bladder, and moderate uptake was seen in the liver, spleen, gastrointestinal tract, and colon (*17,49*). The pancreas and gastrointestinal tract express GRPR (*50*), as bombesin works as a stimulator of pancreatic secretion, similar to gastrin and cholecystokinin release (*51,52*).

Kähkönen et al. (*16*) evaluated the potential of ^{68}Ga-RM2 PET/CT in 14 patients with PC (11 at initial diagnosis and 3 with BCR). The PSA level ranged from 6.2 to 45.0 ng/mL for primary PC and from 0.36 to 282 mg/dL for recurrent PC. The tumors in patients with PC ranged from 12 to 35 mm. The sensitivity, specificity, and accuracy for the detection of primary lesions were 88%, 81%, and 83%, respectively; the sensitivity for the detection of lymph node metastases was 70%. The SUV$_{max}$ and SUV$_{mean}$ (mean ± SD) for histologically confirmed PC were 6.6 ± 4.7 and 5.1 ± 3.7, respectively; these values were statistically higher than those for benign prostate hypertrophy (SUV$_{max}$, 2.4 ± 1.5; SUV$_{mean}$, 1.8 ± 1.2) and normal tissue in the peripheral zone (SUV$_{max}$, 1.3 ± 1.0; SUV$_{mean}$, 1.0 ± 0.9).

We evaluated ^{68}Ga-RM2 with PET/MRI in 29 patients with BCR of PC as well as noncontributory conventional imaging (bone scanning, CT, or MRI). All patients had rising PSA levels (range, 0.3–36.4 ng/mL; mean ± SD, 8.5 ± 9.3 ng/mL). The highest ^{68}Ga-RM2 uptake was observed in the pancreas and bladder, whereas moderate uptake was noted in the esophagus, kidneys, blood pool, stomach, small bowel, and colon. High ^{68}Ga-RM2 uptake (SUV$_{max}$, 12.7 ± 7.8 [range, 2.6–33.5]; SUV$_{mean}$, 5.7 ± 2.5 [range, 1.7–10.8]) corresponded to pelvic lymph nodes (8 patients), retroperitoneal lymph nodes (5 patients), prostate bed (3 patients), seminal vesicle (2 patients), supraclavicular lymph node (2 patients), mesenteric lymph nodes (1 patient), mediastinal lymph node (1 patient), liver (1 patient), lung (1 patient), and bone marrow (1 patient). ^{68}Ga-RM2 PET findings were compatible with recurrent PC in 20 of the 29 patients. MRI identified findings compatible with recurrent PC in 9 of the 29 patients (lymph nodes in 7 patients, prostate bed in 1 patient, lung in 1 patient, and bone marrow in 1 patient). An example from our cohort is shown in Figure 3.

Maina et al. (*23*) evaluated another GRPR antagonist (^{68}Ga-SB3) in 8 patients with breast cancer and 9 patients with PC. All patients had disseminated disease and had received previous therapies. ^{68}Ga-SB3 did not produce adverse effects and identified cancer lesions in 4 of the 8 patients with breast cancer (50%) and 5 of the 9 patients with PC (55%).

Fluorinated PET radiopharmaceuticals targeting GRPR have been used in clinical trials. Sah et al. (*53*) reported the use of the ^{18}F-labeled bombesin analog BAY 864367 in patients with PC. They evaluated 10 patients with biopsy-proven PC (5 with primary PC and 5 with PSA recurrence after radical prostatectomy). Three of the 5 patients with primary disease had BAY 864367 uptake in the prostate, and 2 of the 5 patients with biochemical relapse had a lesion suggestive of recurrence on the BAY 864367 scan. The tumor-to-background
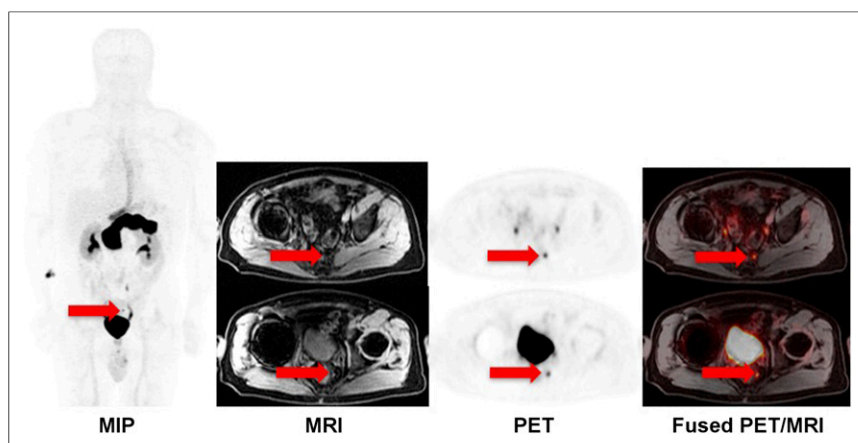

FIGURE 3. 65-y-old man with Gleason 4 + 3 PC treated with prostatectomy, now presenting with PSA of 2.33 ng/mL and negative conventional imaging results. Small perirectal lymph nodes had intense ^{68}Ga-RM2 uptake (arrows). Images were acquired with SIGNA time-of-flight–enabled simultaneous PET/MRI scanner (GE Healthcare). MIP = maximum-intensity projection.

ratio averaged 12.9 ± 7.0, and the reported mean effective dose was 4.3 ± 0.3 mSv/patient (range, 3.7–4.9 mSv).

Isotopes with longer half-lives, such as ^{64}Cu, were also used to label GRPR antagonists (54). Wieser et al. (54) indicated that ^{64}Cu-CB-TE2A-AR06 had favorable characteristics for the imaging of PC, with 3 of 4 cancers being visualized with high contrast and another cancer being visualized with moderate contrast 4 h after injection.

Although encouraging results have been shown for PET radiopharmaceuticals targeting GRPR, the PSMA target for the imaging of PC has been used extensively and with great success recently. PSMA is highly expressed in PC cells in comparison with other PSMA-expressing normal tissues, such as kidney, proximal small intestine, and salivary gland tissues (55). After an initial study with ^{68}Ga-PSMA in patients with PC (56), multiple subsequent publications have indicated that ^{68}Ga-PSMA detects primary and recurrent PC with high sensitivity and specificity (57–60). Therefore, it is important to evaluate GRPR– and PSMA–targeting PET radiopharmaceuticals in the same patients. In a study in which ^{68}Ga-PSMA and ^{68}Ga-RM2 were directly compared, ^{68}Ga-PSMA uptake in malignant lesions (prostate bed, lymph nodes, seminal vesicle, and bone marrow) was not statistically significantly different from ^{68}Ga-RM2 uptake in the same areas (49). That study showed similar diagnostic performances of ^{68}Ga-PSMA and ^{68}Ga-RM2. However, the lack of significant hepatobiliary clearance of ^{68}Ga-RM2 may make small abdominal and pelvic lesions more conspicuous on ^{68}Ga-RM2 images than on ^{68}Ga-PSMA images. Additional work is needed to understand the expression of PSMA and GRPR in different types of PC.

There are limitations of the data related to the use of GRPR-targeting PET peptides, including small sample sizes in studies published to date, limited gold standards, and limited outcome data. Larger studies are needed to confirm preliminary results. As with other PET radiopharmaceuticals, the excretion of these agents into the bladder may be problematic for detecting disease in the prostate gland/bed and, in some cases, in pelvic lymph nodes. However, the administration of furosemide may alleviate this limitation.

The simultaneous PET/MRI scanners introduced into clinical use in recent years (61,62) can provide both functional information and morphologic information about various biologic processes. Compared with PET/CT, simultaneous PET/MRI has advantages resulting from a reduction in radiation exposure, improvements in diagnostic ability attributable to better soft-tissue contrast, and multiparametric MRI techniques (63). A combination of advanced simultaneous PET/MRI scanners and novel specific PET radiopharmaceuticals, such as GRPR antagonists, may be ideal for the detection of PC at initial diagnosis and for evaluation for oligometastatic disease and BCR.

CONCLUSION

Extensive and significant preclinical and translational work as well as promising results from early clinical trials indicate that imaging of the expression of GRPR has the potential to play a significant role in the identification of one biologic process involved in PC.

DISCLOSURE

No potential conflict of interest relevant to this article was reported.

REFERENCES

1. Siegel RL, Miller KD, Jemal A. Cancer statistics, 2016. *CA Cancer J Clin.* 2016;66:7–30.
2. Yu Z, Ananias HJ, Carlucci G, et al. An update of radiolabeled bombesin analogs for gastrin-releasing peptide receptor targeting. *Curr Pharm Des.* 2013;19:3329–3341.
3. Moreno P, Ramos-Álvarez I, Moody TW, Jensen RT. Bombesin related peptides/receptors and their promising therapeutic roles in cancer imaging, targeting and treatment. *Expert Opin Ther Targets.* 2016:1–19.
4. Mansi R, Fleischmann A, Macke HR, Reubi JC. Targeting GRPR in urological cancers: from basic research to clinical application. *Nat Rev Urol.* 2013;10:235–244.
5. Jensen RT, Battey JF, Spindel ER, Benya RV. International Union of Pharmacology. LXVIII. Mammalian bombesin receptors: nomenclature, distribution, pharmacology, signaling, and functions in normal and disease states. *Pharmacol Rev.* 2008;60:1–42.
6. Markwalder R, Reubi JC. Gastrin-releasing peptide receptors in the human prostate: relation to neoplastic transformation. *Cancer Res.* 1999;59:1152–1159.
7. Richter S, Wuest M, Bergman CN, et al. Rerouting the metabolic pathway of ^{18}F-labeled peptides: the influence of prosthetic groups. *Bioconjug Chem.* 2015; 26:201–212.
8. Schweinsberg C, Maes V, Brans L, et al. Novel glycated [^{99m}Tc(CO)$_3$]-labeled bombesin analogues for improved targeting of gastrin-releasing peptide receptor-positive tumors. *Bioconjug Chem.* 2008;19:2432–2439.
9. Dimitrakopoulou-Strauss A, Hohenberger P, Haberkorn U, Macke HR, Eisenhut M, Strauss LG. ^{68}Ga-labeled bombesin studies in patients with gastrointestinal stromal tumors: comparison with ^{18}F-FDG. *J Nucl Med.* 2007;48:1245–1250.
10. Strauss LG, Koczan D, Seiz M, et al. Correlation of the Ga-68-bombesin analog Ga-68-BZH3 with receptor expression in gliomas as measured by quantitative dynamic positron emission tomography (dPET) and gene arrays. *Mol Imaging Biol.* 2012;14:376–383.
11. Baum RP, Prasad V, Frischknecht M, Maecke HR, Reubi JC. Bombesin receptor imaging in various tumors: first results of Ga-68 AMBA PET/CT [abstract]. *Eur J Nucl Med Mol Imaging.* 2007;34(suppl 2):S193.
12. Carlucci G, Kuipers A, Ananias HJK, et al. GRPR-selective PET imaging of prostate cancer using [^{18}F]-lanthionine-bombesin analogs. *Peptides.* 2015;67:45–54.
13. Llinares M, Devin C, Chaloin O, et al. Syntheses and biological activities of potent bombesin receptor antagonists. *J Pept Res.* 1999;53:275–283.
14. Mansi R, Wang X, Forrer F, et al. Evaluation of a 1,4,7,10-tetraazacyclododecane-1,4,7,10-tetraacetic acid-conjugated bombesin-based radioantagonist for the labeling with single-photon emission computed tomography, positron emission tomography, and therapeutic radionuclides. *Clin Cancer Res.* 2009;15:5240–5249.
15. Mansi R, Wang X, Forrer F, et al. Development of a potent DOTA-conjugated bombesin antagonist for targeting GRPr-positive tumours. *Eur J Nucl Med Mol Imaging.* 2011;38:97–107.
16. Kähkönen E, Jambor I, Kemppainen J, et al. In vivo imaging of prostate cancer using [^{68}Ga]-labeled bombesin analog BAY86-7548. *Clin Cancer Res.* 2013;19:5434–5443.
17. Roivainen A, Kähkönen E, Luoto P, et al. Plasma pharmacokinetics, whole-body distribution, metabolism, and radiation dosimetry of ^{68}Ga-bombesin antagonist BAY 86-7548 in healthy men. *J Nucl Med.* 2013;54:867–872.
18. Varasteh Z, Aberg O, Velikyan I, et al. In vitro and in vivo evaluation of a ^{18}F-labeled high affinity NOTA conjugated bombesin antagonist as a PET ligand for GRPR-targeted tumor imaging. *PLoS One.* 2013;8:e81932.
19. Chatalic KLS, Franssen GM, van Weerden WM, et al. Preclinical comparison of Al^{18}F- and ^{68}Ga-labeled gastrin-releasing peptide receptor antagonists for PET imaging of prostate cancer. *J Nucl Med.* 2014;55:2050–2056.
20. Gourni E, Mansi R, Jamous M, et al. N-terminal modifications improve the receptor affinity and pharmacokinetics of radiolabeled peptidic gastrin-releasing peptide receptor antagonists: examples of ^{68}Ga- and ^{64}Cu-labeled peptides for PET imaging. *J Nucl Med.* 2014;55:1719–1725.
21. Abiraj K, Mansi R, Tamma ML, et al. Bombesin antagonist–based radioligands for translational nuclear imaging of gastrin-releasing peptide receptor–positive tumors. *J Nucl Med.* 2011;52:1970–1978.
22. Gourni E, Del Pozzo L, Kheirallah E, et al. Copper-64 labeled macrobicyclic sarcophagine coupled to a GRP receptor antagonist shows great promise for PET imaging of prostate cancer. *Mol Pharm.* 2015;12:2781–2790.
23. Maina T, Bergsma H, Kulkarni HR, et al. Preclinical and first clinical experience with the gastrin-releasing peptide receptor-antagonist [^{68}Ga]SB3 and PET/CT. *Eur J Nucl Med Mol Imaging.* 2016;43:964–973.
24. Nanda PK, Pandey U, Bottenus BN, et al. Bombesin analogues for gastrin-releasing peptide receptor imaging. *Nucl Med Biol.* 2012;39:461–471.
25. Mansi R, Abiraj K, Wang X, et al. Evaluation of three different families of bombesin receptor radioantagonists for targeted imaging and therapy of gastrin releasing peptide receptor (GRP-R) positive tumors. *J Med Chem.* 2015;58:682–691.

26. Lantry LE, Cappelletti E, Maddalena ME, et al. ^{177}Lu-AMBA: synthesis and characterization of a selective ^{177}Lu-labeled GRP-R agonist for systemic radiotherapy of prostate cancer. *J Nucl Med.* 2006;47:1144–1152.

27. Liu Y, Hu X, Liu H, et al. A comparative study of radiolabeled bombesin analogs for the PET imaging of prostate cancer. *J Nucl Med.* 2013;54:2132–2138.

28. Cescato R, Maina T, Nock B, et al. Bombesin receptor antagonists may be preferable to agonists for tumor targeting. *J Nucl Med.* 2008;49:318–326.

29. Nanda PK, Wienhoff BE, Rold TL, et al. Positron-emission tomography (PET) imaging agents for diagnosis of human prostate cancer: agonist vs. antagonist ligands. *In Vivo.* 2012;26:583–592.

30. Yang M, Gao H, Zhou Y, et al. F-labeled GRPR agonists and antagonists: a comparative study in prostate cancer imaging. *Theranostics.* 2011;1:220–229.

31. Li ZB, Wu Z, Chen K, Ryu EK, Chen X. ^{18}F-labeled BBN-RGD heterodimer for prostate cancer imaging. *J Nucl Med.* 2008;49:453–461.

32. Liu Z, Li ZB, Cao Q, Liu S, Wang F, Chen X. Small-animal PET of tumors with ^{64}Cu-labeled RGD-bombesin heterodimer. *J Nucl Med.* 2009;50:1168–1177.

33. Zhou Z, Wagh NK, Ogbomo SM, et al. Synthesis and in vitro and in vivo evaluation of hypoxia-enhanced ^{111}In-bombesin conjugates for prostate cancer imaging. *J Nucl Med.* 2013;54:1605–1612.

34. Bandari RP, Jiang Z, Reynolds TS, et al. Synthesis and biological evaluation of copper-64 radiolabeled [DUPA-6-Ahx-(NODAGA)-5-Ava-BBN(7–14)NH$_2$], a novel bivalent targeting vector having affinity for two distinct biomarkers (GRPr/PSMA) of prostate cancer. *Nucl Med Biol.* 2014;41:355–363.

35. Kroll C, Mansi R, Braun F, Dobitz S, Maecke HR, Wennemers H. Hybrid bombesin analogues: combining an agonist and an antagonist in defined distances for optimized tumor targeting. *J Am Chem Soc.* 2013;135:16793–16796.

36. Isbarn H, Wanner M, Salomon G, et al. Long-term data on the survival of patients with prostate cancer treated with radical prostatectomy in the prostate-specific antigen era. *BJU Int.* 2010;106:37–43.

37. Beer AJ, Eiber M, Souvatzoglou M, Schwaiger M, Krause BJ. Radionuclide and hybrid imaging of recurrent prostate cancer. *Lancet Oncol.* 2011;12:181–191.

38. Oyen RH, Van Poppel HP, Ameye FE, Van de Voorde WA, Baert AL, Baert LV. Lymph node staging of localized prostatic carcinoma with CT and CT-guided fine-needle aspiration biopsy: prospective study of 285 patients. *Radiology.* 1994;190:315–322.

39. Jadvar H. Prostate cancer: PET with ^{18}F-FDG, [18]F- or ^{11}C-acetate, and [18]F- or ^{11}C-choline. *J Nucl Med.* 2011;52:81–89.

40. Jadvar H. Molecular imaging of prostate cancer: PET radiotracers. *AJR.* 2012;199:278–291.

41. Minamimoto R, Uemura H, Sano F, et al. The potential of FDG-PET/CT for detecting prostate cancer in patients with an elevated serum PSA level. *Ann Nucl Med.* 2011;25:21–27.

42. Oyama N, Miller TR, Dehdashti F, et al. ^{11}C-acetate PET imaging of prostate cancer: detection of recurrent disease at PSA relapse. *J Nucl Med.* 2003;44:549–555.

43. Picchio M, Messa C, Landoni C, et al. Value of [^{11}C]choline-positron emission tomography for re-staging prostate cancer: a comparison with [^{18}F]fluorodeoxyglucose-positron emission tomography. *J Urol.* 2003;169:1337–1340.

44. Albrecht S, Buchegger F, Soloviev D, et al. ^{11}C-acetate PET in the early evaluation of prostate cancer recurrence. *Eur J Nucl Med Mol Imaging.* 2007;34:185–196.

45. Wachter S, Tomek S, Kurtaran A, et al. ^{11}C-acetate positron emission tomography imaging and image fusion with computed tomography and magnetic resonance imaging in patients with recurrent prostate cancer. *J Clin Oncol.* 2006;24:2513–2519.

46. Beheshti M, Haim S, Zakavi R, et al. Impact of ^{18}F-choline PET/CT in prostate cancer patients with biochemical recurrence: influence of androgen deprivation therapy and correlation with PSA kinetics. *J Nucl Med.* 2013;54:833–840.

47. Nanni C, Schiavina R, Boschi S, et al. Comparison of ^{18}F-FACBC and ^{11}C-choline PET/CT in patients with radically treated prostate cancer and biochemical relapse: preliminary results. *Eur J Nucl Med Mol Imaging.* 2013;40(suppl):S11–S17.

48. Turkbey B, Mena E, Shih J, et al. Localized prostate cancer detection with ^{18}F FACBC PET/CT: comparison with MR imaging and histopathologic analysis. *Radiology.* 2014;270:849–856.

49. Minamimoto R, Hancock S, Schneider B, et al. Pilot comparison of ^{68}Ga-RM2 PET and ^{68}Ga-PSMA-11 PET in patients with biochemically recurrent prostate cancer. *J Nucl Med.* 2016;57:557–562.

50. Nishino H, Tsunoda Y, Owyang C. Mammalian bombesin receptors are coupled to multiple signal transduction pathways in pancreatic acini. *Am J Physiol.* 1998;274:G525–G534.

51. Polak JM, Hobbs S, Bloom SR, Solcia E, Pearse AGE. Distribution of a bombesin-like peptide in human gastrointestinal tract. *Lancet.* 1976;1:1109–1110.

52. Erspamer V, Improta G, Melchiorri P, Sopranzi N. Evidence of cholecystokinin release by bombesin in the dog. *Br J Pharmacol.* 1974;52:227–232.

53. Sah B-R, Burger IA, Schibli R, et al. Dosimetry and first clinical evaluation of the new ^{18}F-radiolabeled bombesin analogue BAY 864367 in patients with prostate cancer. *J Nucl Med.* 2015;56:372–378.

54. Wieser G, Mansi R, Grosu AL, et al. Positron emission tomography (PET) imaging of prostate cancer with a gastrin releasing peptide receptor antagonist: from mice to men. *Theranostics.* 2014;4:412–419.

55. Sweat SD, Pacelli A, Murphy GP, Bostwick DG. Prostate-specific membrane antigen expression is greatest in prostate adenocarcinoma and lymph node metastases. *Urology.* 1998;52:637–640.

56. Afshar-Oromieh A, Malcher A, Eder M, et al. PET imaging with a [^{68}Ga]gallium-labelled PSMA ligand for the diagnosis of prostate cancer: biodistribution in humans and first evaluation of tumour lesions. *Eur J Nucl Med Mol Imaging.* 2013;40:486–495.

57. Afshar-Oromieh A, Zechmann CM, Malcher A, et al. Comparison of PET imaging with a ^{68}Ga-labelled PSMA ligand and ^{18}F-choline-based PET/CT for the diagnosis of recurrent prostate cancer. *Eur J Nucl Med Mol Imaging.* 2014;41:11–20.

58. Afshar-Oromieh A, Haberkorn U, Schlemmer HP, et al. Comparison of PET/CT and PET/MRI hybrid systems using a ^{68}Ga-labelled PSMA ligand for the diagnosis of recurrent prostate cancer: initial experience. *Eur J Nucl Med Mol Imaging.* 2014;41:887–897.

59. Eiber M, Maurer T, Souvatzoglou M, et al. Evaluation of hybrid ^{68}Ga-PSMA ligand PET/CT in 248 patients with biochemical recurrence after radical prostatectomy. *J Nucl Med.* 2015;56:668–674.

60. Eiber M, Weirich G, Holzapfel K, et al. Simultaneous ^{68}Ga-PSMA HBED-CC PET/MRI improves the localization of primary prostate cancer. *Eur Urol.* January 18, 2016 [Epub ahead of print].

61. Delso G, Fürst S, Jakoby B, et al. Performance measurements of the Siemens mMR integrated whole-body PET/MR scanner. *J Nucl Med.* 2011;52:1914–1922.

62. Iagaru A, Mittra E, Minamimoto R, et al. Simultaneous whole-body time-of-flight ^{18}F-FDG PET/MRI: a pilot study comparing SUV$_{max}$ with PET/CT and assessment of MR image quality. *Clin Nucl Med.* 2015;40:1–8.

63. Antoch G, Bockisch A. Combined PET/MRI: a new dimension in whole-body oncology imaging? *Eur J Nucl Med Mol Imaging.* 2009;36(suppl):S113–S120.